

Distributed Iteratively Quantized Kalman Filtering for Wireless Sensor Networks

Eric J. Msechu*, Stergios I. Roumeliotis[†], Alejandro Ribeiro*, and Georgios B. Giannakis* (contact author)

Abstract— Estimation and tracking of generally nonstationary Markov processes is of paramount importance for applications such as localization and navigation. In this context, *ad hoc* wireless sensor networks (WSNs) offer distributed Kalman filtering (KF) based algorithms with documented merits over centralized alternatives. Adhering to the limited power and bandwidth resources WSNs must operate with, this paper introduces a novel distributed KF estimator based on quantized measurement innovations. The quantized observations and the distributed nature of the iteratively quantized KF algorithm are amenable to the resource constraints of the *ad hoc* WSNs. Analysis and simulations show that KF-like tracking based on m bits of iteratively quantized innovations communicated among sensors exhibits MSE performance identical to a KF based on analog-amplitude observations applied to an observation model with noise variance increased by a factor of $[1 - (1 - 2/\pi)^m]^{-1}$. With minimal communication overhead, the mean-square error (MSE) of the distributed KF-like tracker based on 2-3 bits is almost indistinguishable from that of the clairvoyant KF.

Keywords: wireless sensor networks, distributed state estimation, Kalman filtering, quantized observations, limited-rate communication.

I. INTRODUCTION

Consider an *ad-hoc* wireless sensor network (WSN) deployed to track a Markov stochastic process. Each sensor node acquires observations which are noisy linear transformation of a common state. The sensors then transmit observations to each other in order to form a state estimate. If observations were available at a common location, minimum mean-square error (MMSE) estimates could be obtained using a Kalman filter (KF). However, since observations are distributed in space and there is limited communication bandwidth, the observations have to be quantized before transmission. Thus, the original estimation problem is transformed into distributed state estimation based on quantized observations.

Quantizing observations to estimate a parameter of interest, is *not* the same as quantizing a signal for later reconstruction [3]. Instead of a reconstruction algorithm, the objective is finding, e.g., MMSE optimal, estimators using quantized observations [7]. Furthermore, optimal quantizers for reconstruction are, generally, different from optimal quantizers for estimation.

State estimation using quantized observations is a non-linear estimation problem that can be solved using e.g., unscented (U)KFs [4] or particle filters [2]. It was shown in [8] that if

Prepared through collaborative participation in the Communication and Networks Consortium sponsored by the U. S. Army Research Lab under the Collaborative Technology Alliance Program, Cooperative Agreement DAAD19-01-2-0011. The U. S. Government is authorized to reproduce and distribute reprints for Government purposes notwithstanding any copyright notation thereon.

*Dept. of ECE, Univ. of Minnesota, 200 Union Street SE, Minneapolis, MN 55455, Email: {msechu,aribeiro,georgios}@ece.umn.edu, Tel/fax: (612) 626-7781/ 625-4583;

[†]Dept. of CSE, Univ. of Minnesota, 200 Union Street SE, Minneapolis, MN 55455, Email: stergios@cs.umn.edu, Tel/fax: (612) 626-7507/ (612) 625-0572.

quantized observations are generated as the sign of the innovation (SoI) sequence, a filter with complexity and performance very close to the clairvoyant KF based on the analog-amplitude observations can be derived. Even though promising, the approach of [8] is limited to a particular 1-bit per observation quantizer.

This paper builds on and considerably broadens the scope of [8] by addressing the middle ground between estimators based on severely quantized (1-bit) data and those based on unquantized data. The end result is a quantizer-estimator that offers desirable trade-offs between bandwidth requirements (dictating the number of quantization bits used for inter-sensor communications) and overall tracking performance (assessed by the mean-square state estimation error).

II. MODELS AND PROBLEM STATEMENT

Consider an ad-hoc WSN whose K sensor nodes $\{S_k\}_{k=1}^K$ estimate a multivariate real-valued random process $\mathbf{x}_c(t) \in \mathbb{R}^p$, where $^\circ$ denotes continuous-time. The state equation is given as

$$\dot{\mathbf{x}}_c(t) = \mathbf{A}_c(t)\mathbf{x}_c(t) + \mathbf{u}_c(t) \quad (1)$$

where $\mathbf{A}_c(t) \in \mathbb{R}^{p \times p}$ denotes the state transition matrix and $\mathbf{u}_c(t)$ is assumed zero-mean white Gaussian process with covariance matrix $E\{\mathbf{u}_c(t)\mathbf{u}_c^T(\tau)\} = \mathbf{C}_{u_c}(t)\delta_c(t - \tau)$.

The k -th sensor S_k records scalar observations

$$y_{c,k}(t) = \mathbf{h}_{c,k}^T(t)\mathbf{x}_c(t) + v_{c,k}(t) \quad (2)$$

where $\mathbf{h}_{c,k}(t) \in \mathbb{R}^p$ denotes the regression vector, and $v_{c,k}(t)$ is a temporally and spatially white zero-mean Gaussian noise process with covariance $E\{v_{c,k}(t)v_{c,l}(\tau)\} = c_{v_c}(t)\delta_c(t - \tau)\delta_{kl}$. It is further assumed that $\mathbf{u}_c(t)$ is independent of both $v_{c,k}(t)$ and $\mathbf{x}_c(t_0)$, where t_0 is an arbitrary initial reference time.

The discrete-time counterpart of (1) is obtained using the definitions $\Phi(t_2, t_1) := \exp\left[\int_{t_1}^{t_2} \mathbf{A}_c(t)dt\right]$, $\mathbf{x}(n) := \mathbf{x}_c(nT_s)$, and $\mathbf{u}(n) := \int_{(n-1)T_s}^{nT_s} \Phi(nT_s, \tau)\mathbf{u}_c(\tau)d\tau$ where T_s is the sampling period. From [6, Section 4.9] the discrete-time state is

$$\mathbf{x}(n) = \mathbf{A}(n)\mathbf{x}(n-1) + \mathbf{u}(n) \quad (3)$$

where $\mathbf{u}(n)$ is zero-mean white Gaussian with covariance matrix $\mathbf{C}_u(n) = \int_{(n-1)T_s}^{nT_s} \Phi(nT_s, \tau)\mathbf{C}_{u_c}(\tau)\Phi^T(nT_s, \tau)d\tau$; and $\mathbf{A}(n) := \Phi(nT_s, (n-1)T_s)$. The discrete-time counterpart of the observation equation (2) is obtained as

$$y_k(n) = \mathbf{h}_k^T(n)\mathbf{x}(n) + v_k(n) \quad (4)$$

where $y_k(n) := y_{c,k}(nT_s)$ is obtained by uniform sampling of (2) followed by low- or band-pass filtering with bandwidth T_s , leading to zero-mean white Gaussian discrete-time noise $v_k(n)$ with variance $c_v(n) = c_{v_c}(nT_s)/T_s$ [6, Section 4.9].

Supposing that $\mathbf{A}(n)$, $\mathbf{C}_u(n)$, $\mathbf{h}_k(n)$ and $c_v(n)$ are available $\forall n, k$, the goal of the WSN is for each sensor S_k to form

an estimate of $\mathbf{x}(n)$. Estimating $\mathbf{x}(n)$ necessitates each sensor S_k to communicate $y_k(n)$ to all other sensors $\{S_l\}_{l=1, l \neq k}^K$. Communication takes place over the shared wireless channel that we assume can afford transmission of a single packet of m bits per time slot n . This leads to a one-to-one correspondence between time n and sensor index k and allows us to drop the sensor argument k in (4).

A. MMSE estimation with quantized observations

Let the quantization at time index n be defined as $b(n) := \mathbf{q}_n[y(n)]$, then given current and past messages $\mathbf{b}_{1:n} := \{b(1), b(2), \dots, b(n)\}$ we are interested in estimates $\hat{\mathbf{x}}(n|\mathbf{b}_{1:n})$ of the state $\mathbf{x}(n)$ using the information in $\mathbf{b}_{1:n}$. The mean-square error (MSE) of the estimator is obtained as the trace of the error covariance matrix (ECM) $\mathbf{M}(n|\mathbf{b}_{1:n}) := \mathbb{E}\{[\hat{\mathbf{x}}(n|\mathbf{b}_{1:n}) - \mathbf{x}(n)][\hat{\mathbf{x}}(n|\mathbf{b}_{1:n}) - \mathbf{x}(n)]^T\}$, i.e., $\text{tr}\{\mathbf{M}(n|\mathbf{b}_{1:n})\}$. The MMSE estimator is the conditional mean, see e.g., [6, Chapter 5],

$$\hat{\mathbf{x}}(n|\mathbf{b}_{1:n}) = \mathbb{E}\{\mathbf{x}(n)|\mathbf{b}_{1:n}\} := \int_{\mathbb{R}^p} \mathbf{x}(n) p[\mathbf{x}(n)|\mathbf{b}_{1:n}] d\mathbf{x}(n). \quad (5)$$

To obtain a closed-form expression for $\hat{\mathbf{x}}(n|\mathbf{b}_{1:n})$, the posterior distribution $p[\mathbf{x}(n)|\mathbf{b}_{1:n}]$ has to be known and the integral in (5) needs to be computed. In principle, $p[\mathbf{x}(n)|\mathbf{b}_{1:n}]$ can be obtained recursively using Bayes' rule as follows:

$$p[\mathbf{x}(n)|\mathbf{b}_{1:n}] = p[\mathbf{x}(n)|\mathbf{b}_{1:n-1}] \frac{\Pr\{b(n)|\mathbf{x}(n), \mathbf{b}_{1:n-1}\}}{\Pr\{b(n)|\mathbf{b}_{1:n-1}\}} \quad (6)$$

where $\Pr\{b(n)|\mathbf{x}(n), \mathbf{b}_{1:n-1}\}$ and $\Pr\{b(n)|\mathbf{b}_{1:n-1}\}$ depend on the quantization rule $\mathbf{q}_n[y(n)]$. If $p[\mathbf{x}(n-1)|\mathbf{b}_{1:n-1}]$ is known, the prior pdf $p[\mathbf{x}(n)|\mathbf{b}_{1:n-1}]$ can be obtained as

$$p[\mathbf{x}(n)|\mathbf{b}_{1:n-1}] = \int_{\mathbb{R}^p} p[\mathbf{x}(n)|\mathbf{x}(n-1), \mathbf{b}_{1:n-1}] p[\mathbf{x}(n-1)|\mathbf{b}_{1:n-1}] d\mathbf{x}(n-1) \quad (7)$$

where due to Gaussian and Markov properties of the random process $\mathbf{x}(n)$ in (3), $p[\mathbf{x}(n)|\mathbf{x}(n-1), \mathbf{b}_{1:n-1}] = p[\mathbf{x}(n)|\mathbf{x}(n-1)] = \mathcal{N}[\mathbf{x}(n); \mathbf{A}(n)\mathbf{x}(n-1), \mathbf{C}_u(n)]$.

If $b(n) = y(n)$, i.e., un-quantized observations are used, both conditional pdfs in (7) and (6) are Gaussian and it suffices to propagate their means and covariance matrices only. This leads to the following Kalman filter recursions [6, Chapter 5.3]:

[P1] KF prediction step. Given the previous estimate $\hat{\mathbf{x}}(n-1|y_{1:n-1})$ and its ECM $\mathbf{M}(n-1|y_{1:n-1})$, the predicted estimate $\hat{\mathbf{x}}(n|y_{1:n-1}) := \mathbb{E}\{\mathbf{x}(n)|y_{1:n-1}\}$ and its ECM $\mathbf{M}(n|y_{1:n-1}) := \mathbb{E}\{[\hat{\mathbf{x}}(n|y_{1:n-1}) - \mathbf{x}(n)][\hat{\mathbf{x}}(n|y_{1:n-1}) - \mathbf{x}(n)]^T\}$ are obtained as

$$\hat{\mathbf{x}}(n|y_{1:n-1}) = \mathbf{A}(n)\hat{\mathbf{x}}(n-1|y_{1:n-1}) \quad (8)$$

$$\mathbf{M}(n|y_{1:n-1}) = \mathbf{A}(n)\mathbf{M}(n-1|y_{1:n-1})\mathbf{A}^T(n) + \mathbf{C}_u(n). \quad (9)$$

[C1] KF correction step. Consider the predicted data $\mathbb{E}\{y(n)|y_{1:n-1}\} := \hat{y}(n|y_{1:n-1}) = \mathbf{h}^T(n)\hat{\mathbf{x}}(n|y_{1:n-1})$ and their innovation $\tilde{y}(n|y_{1:n-1}) := y(n) - \hat{y}(n|y_{1:n-1})$. Then

$\hat{\mathbf{x}}(n|y_{1:n})$ in (5) and its ECM $\mathbf{M}(n|y_{1:n})$ are given as

$$\hat{\mathbf{x}}(n|y_{1:n}) = \hat{\mathbf{x}}(n|y_{1:n-1}) + \frac{\mathbf{M}(n|y_{1:n-1})\mathbf{h}(n)}{\mathbf{h}^T(n)\mathbf{M}(n|y_{1:n-1})\mathbf{h}(n) + c_v(n)} \tilde{y}(n|y_{1:n-1}) \quad (10)$$

$$\mathbf{M}(n|y_{1:n}) = \mathbf{M}(n|y_{1:n-1}) - \frac{\mathbf{M}(n|y_{1:n-1})\mathbf{h}(n)\mathbf{h}^T(n)\mathbf{M}(n|y_{1:n-1})}{\mathbf{h}^T(n)\mathbf{M}(n|y_{1:n-1})\mathbf{h}(n) + c_v(n)}. \quad (11)$$

Computations for the KF iteration in [P1]-[C1] require a few algebraic operations per time-step n whereas (6) - (7) require: (i) multi-dimensional numerical integration to obtain the predicted pdf $p[\mathbf{x}(n)|\mathbf{b}_{1:n-1}]$ in (7) and to evaluate the expectation in (5); and (ii) numerical update of the posterior pdf $p[\mathbf{x}(n)|\mathbf{b}_{1:n}]$ in (6). This high computational cost is inherent to non-linear models (non-linearity in this paper is due to quantization of the observations) and motivates lower complexity approximations.

By using a Gaussian approximation for the prior pdf $p[\mathbf{x}(n)|\mathbf{b}_{1:n-1}]$, see e.g., [5], tracking of the potentially intractable pdf $p[\mathbf{x}(n)|\mathbf{b}_{1:n-1}]$ simplifies to keeping track of its mean and covariance matrix. This leads to iterations similar to [P1]-[C1] as detailed in the next section.

III. DISTRIBUTED ITERATIVELY QUANTIZED KALMAN FILTER

To design the iteratively quantized Kalman filter (IQKF), let sensors rely on m -bit binary messages $\mathbf{b}(n) := \mathbf{b}^{(1:m)}(n) := [b^{(1)}(n), \dots, b^{(m)}(n)]$, with the i -th bit $b^{(i)}(n)$ defined as the sign of innovations [cf. (13)] conditioned on the previous messages $\mathbf{b}_{1:n-1} := [b(1), \dots, b(n-1)]$ and previous bits $\mathbf{b}^{(1:i-1)}(n) := [b^{(1)}(n), \dots, b^{(i-1)}(n)]$ of the current (n -th) message. Specifically, let

$$\begin{aligned} \hat{y}^{(0)}(n|\mathbf{b}_{1:n-1}) &:= \hat{y}(n|\mathbf{b}_{1:n-1}) = \mathbb{E}\{y(n)|\mathbf{b}_{1:n-1}\} \\ \hat{y}^{(i)}(n|\mathbf{b}_{1:n-1}) &:= \mathbb{E}\{y(n)|\mathbf{b}_{1:n-1}, \mathbf{b}^{(1:i)}(n)\}, \text{ for } i \geq 1 \end{aligned} \quad (12)$$

stand for MMSE estimates of $y(n)$ using past messages $\mathbf{b}_{1:n-1}$ and the first i bits of the current message denoted as $\mathbf{b}^{(1:i)}(n)$. The i -th bit of the current message, $b^{(i)}(n)$, is defined as

$$b^{(i)}(n) := \text{sign}[y(n) - \hat{y}^{(i-1)}(n|\mathbf{b}_{1:n-1})] := \text{sign}[\tilde{y}^{(i-1)}(n|\mathbf{b}_{1:n-1})]. \quad (13)$$

Our goal is to iteratively compute the estimates

$$\hat{\mathbf{x}}^{(i)}(n|\mathbf{b}_{1:n-1}) := \mathbb{E}\{\mathbf{x}(n)|\mathbf{b}_{1:n-1}, \mathbf{b}^{(1:i)}(n)\} \quad (14)$$

based on $\hat{\mathbf{x}}^{(i-1)}(n|\mathbf{b}_{1:n-1})$ and $b^{(i)}(n)$. When using m bits, $\mathbf{b}^{(1:m)}(n)$, we will refer to the resulting algorithm as m-IQKF.

A possible option for defining the quantizer would be to set $\hat{y}^{(i)}(n|\mathbf{b}_{1:n-1})$ equal to $\mathbf{h}^T(n)\hat{\mathbf{x}}^{(i)}(n|\mathbf{b}_{1:n-1})$. However, $\hat{y}^{(i)}(n|\mathbf{b}_{1:n-1}) \neq \mathbf{h}^T(n)\hat{\mathbf{x}}^{(i)}(n|\mathbf{b}_{1:n-1})$ if $i \geq 1$ as explained next. Using the observations (4), the definitions of $\hat{y}^{(i)}(n|\mathbf{b}_{1:n-1})$ in (12), and $\hat{\mathbf{x}}^{(i)}(n|\mathbf{b}_{1:n-1})$ in (14), we obtain

$$\begin{aligned} \hat{y}^{(i)}(n|\mathbf{b}_{1:n-1}) &= \mathbb{E}\{\mathbf{h}^T(n)\mathbf{x}(n) + v(n)|\mathbf{b}_{1:n-1}, \mathbf{b}^{(1:i)}(n)\} \\ &= \mathbf{h}^T(n)\hat{\mathbf{x}}^{(i)}(n|\mathbf{b}_{1:n-1}) + \mathbb{E}\{v(n)|\mathbf{b}_{1:n-1}, \mathbf{b}^{(1:i)}(n)\}. \end{aligned} \quad (15)$$

The noise estimate $\mathbb{E}\{v(n)|\mathbf{b}_{1:n-1}, \mathbf{b}^{(1:i)}(n)\}$ is not necessarily zero - see also (22). Therefore, in order to obtain $\hat{y}^{(i)}(n|\mathbf{b}_{1:n-1})$ we need $\hat{\mathbf{x}}^{(i)}(n|\mathbf{b}_{1:n-1})$ as well as $\mathbb{E}\{v(n)|\mathbf{b}_{1:n-1}, \mathbf{b}^{(1:i)}(n)\}$ which is achieved by augmenting the state vector $\mathbf{x}(n)$ with the noise term $v(n)$ as described in the next section.

A. State augmentation

Through state augmentation the estimates $E\{v(n)|\mathbf{b}_{1:n-1}, \mathbf{b}^{(1:i)}(n)\}$ can be obtained so that the predicted observation $\hat{y}^{(i)}(n|\mathbf{b}_{1:n-1})$ in (15) can be evaluated. Specifically, let $\check{\mathbf{x}}(n) := [\mathbf{x}^T(n), v(n)]^T$, $\check{\mathbf{u}}(n) := [\mathbf{u}^T(n), v(n)]^T$, $\check{\mathbf{h}}(n) := [\mathbf{h}^T(n), 1]^T$, and $\check{\mathbf{A}}(n)$ defined with $\mathbf{A}(n)$ as the leading $p \times p$ submatrix and with zeros in all other entries; then model in (3)-(4) can be rewritten as

$$\check{\mathbf{x}}(n) = \check{\mathbf{A}}(n)\check{\mathbf{x}}(n-1) + \check{\mathbf{u}}(n) \quad (16)$$

$$\check{y}(n) = \check{\mathbf{h}}^T(n)\check{\mathbf{x}}(n) + \check{v}(n) \quad (17)$$

where the new observation noise $\check{v}(n) = 0$, $\forall n$ (by construction). Note that the covariance matrix of the augmented driving noise is a block-diagonal matrix $\mathbf{C}_{\check{\mathbf{u}}}(n) \in \mathbb{R}^{(p+1) \times (p+1)}$ with $[\mathbf{C}_{\check{\mathbf{u}}}(n)]_{1:p,1:p} = \mathbf{C}_{\mathbf{u}}(n)$ and $[\mathbf{C}_{\check{\mathbf{u}}}(n)]_{p+1,p+1} = c_v(n)$.

The augmented state formulation (16)-(17) increases the dimension of the state vector but is otherwise equivalent to (3)-(4). However, it has the appealing property that MMSE estimates of the augmented state $\check{\mathbf{x}}(n)$ contain MMSE estimates of the original state $\mathbf{x}(n)$ and of the observation noise $v(n)$ which allows computation of $\hat{y}^{(i)}(n|\mathbf{b}_{1:n-1})$ in (12) as follows. Since $\check{y}(n) = \check{\mathbf{h}}^T(n)\check{\mathbf{x}}(n) = \mathbf{h}^T(n)\mathbf{x}(n) + v(n) = y(n)$, it follows that $\hat{y}^{(i)}(n|\mathbf{b}_{1:n-1}) = \hat{\check{y}}^{(i)}(n|\mathbf{b}_{1:n-1}) = \check{\mathbf{h}}^T(n)\hat{\check{\mathbf{x}}}^{(i)}(n|\mathbf{b}_{1:n-1})$ where $\hat{\check{\mathbf{x}}}^{(i)}(n|\mathbf{b}_{1:n-1}) = E\{\check{\mathbf{x}}(n)|\mathbf{b}_{1:n-1}, \mathbf{b}^{(1:i)}(n)\}$ and $\hat{\check{y}}^{(i)}(n|\mathbf{b}_{1:n-1}) = E\{\check{y}(n)|\mathbf{b}_{1:n-1}, \mathbf{b}^{(1:i)}(n)\}$. Using the augmented state model, we obtain the MMSE estimates in (14) using the algorithm detailed in Proposition 1.

Proposition 1 Consider the augmented state space model in (16)-(17). Define the augmented state estimates $\hat{\check{\mathbf{x}}}(n|\mathbf{b}_{1:n-1}) := E\{\check{\mathbf{x}}(n)|\mathbf{b}_{1:n-1}\}$ and $\hat{\check{\mathbf{x}}}^{(i-1)}(n|\mathbf{b}_{1:n-1}) := E\{\check{\mathbf{x}}(n)|\mathbf{b}_{1:n-1}, \mathbf{b}^{(1:i-1)}(n)\}$. Let $\check{\mathbf{M}}(n|\mathbf{b}_{1:n-1}) := E\{[\hat{\check{\mathbf{x}}}(n|\mathbf{b}_{1:n-1}) - \check{\mathbf{x}}(n)][\hat{\check{\mathbf{x}}}(n|\mathbf{b}_{1:n-1}) - \check{\mathbf{x}}(n)]^T\}$ and $\check{\mathbf{M}}^{(i-1)}(n|\mathbf{b}_{1:n-1}) := E\{[\hat{\check{\mathbf{x}}}^{(i-1)}(n|\mathbf{b}_{1:n-1}) - \check{\mathbf{x}}(n)][\hat{\check{\mathbf{x}}}^{(i-1)}(n|\mathbf{b}_{1:n-1}) - \check{\mathbf{x}}(n)]^T\}$ denote the corresponding ECMs for $i = 1, \dots, m$. Construct the messages $\mathbf{b}^{(1:m)}(n)$ in (13) as $b^{(i)}(n) := \text{sign}[y(n) - \check{\mathbf{h}}^T(n)\hat{\check{\mathbf{x}}}^{(i-1)}(n|\mathbf{b}_{1:n-1})]$.

The estimate $\hat{\check{\mathbf{x}}}^{(i)}(n|\mathbf{b}_{1:n-1})$ is obtained from the recursion:

[P2] Given the previous estimate $\hat{\check{\mathbf{x}}}(n-1|\mathbf{b}_{1:n-1})$ and its ECM $\check{\mathbf{M}}(n-1|\mathbf{b}_{1:n-1})$, form

$$\hat{\check{\mathbf{x}}}(n|\mathbf{b}_{1:n-1}) = \check{\mathbf{A}}(n)\hat{\check{\mathbf{x}}}(n-1|\mathbf{b}_{1:n-1}) \quad (18)$$

$$\check{\mathbf{M}}(n|\mathbf{b}_{1:n-1}) = \check{\mathbf{A}}(n)\check{\mathbf{M}}(n-1|\mathbf{b}_{1:n-1})\check{\mathbf{A}}^T(n) + \mathbf{C}_{\check{\mathbf{u}}}(n) \quad (19)$$

[C2] Assuming that $p[\check{\mathbf{x}}(n)|\mathbf{b}_{1:n-1}, \mathbf{b}^{(1:i-1)}(n)] = \mathcal{N}[\check{\mathbf{x}}(n); \hat{\check{\mathbf{x}}}^{(i-1)}(n|\mathbf{b}_{1:n-1}), \check{\mathbf{M}}^{(i-1)}(n|\mathbf{b}_{1:n-1})]$, the MMSE estimate $\hat{\check{\mathbf{x}}}^{(i)}(n|\mathbf{b}_{1:n-1}) := E\{\check{\mathbf{x}}(n)|\mathbf{b}_{1:n-1}, \mathbf{b}^{(1:i)}(n)\}$ and the corresponding ECM $\check{\mathbf{M}}^{(i)}(n|\mathbf{b}_{1:n-1})$ are obtained iteratively from

$$\hat{\check{\mathbf{x}}}^{(i)}(n|\mathbf{b}_{1:n-1}) = \hat{\check{\mathbf{x}}}^{(i-1)}(n|\mathbf{b}_{1:n-1}) + \sqrt{\frac{2}{\pi}} \frac{\check{\mathbf{M}}^{(i-1)}(n|\mathbf{b}_{1:n-1})\check{\mathbf{h}}(n)}{\sqrt{\check{\mathbf{h}}^T(n)\check{\mathbf{M}}^{(i-1)}(n|\mathbf{b}_{1:n-1})\check{\mathbf{h}}(n)}} b^{(i)}(n) \quad (20)$$

$$\check{\mathbf{M}}^{(i)}(n|\mathbf{b}_{1:n-1}) = \check{\mathbf{M}}^{(i-1)}(n|\mathbf{b}_{1:n-1}) - \frac{2}{\pi} \frac{\check{\mathbf{M}}^{(i-1)}(n|\mathbf{b}_{1:n-1})\check{\mathbf{h}}(n)\check{\mathbf{h}}^T(n)\check{\mathbf{M}}^{(i-1)}(n|\mathbf{b}_{1:n-1})}{\check{\mathbf{h}}^T(n)\check{\mathbf{M}}^{(i-1)}(n|\mathbf{b}_{1:n-1})\check{\mathbf{h}}(n)} \quad (21)$$

where we used the definitions $\hat{\check{\mathbf{x}}}^{(0)}(n|\mathbf{b}_{1:n-1}) := \hat{\check{\mathbf{x}}}(n|\mathbf{b}_{1:n-1})$ and $\check{\mathbf{M}}^{(0)}(n|\mathbf{b}_{1:n-1}) := \check{\mathbf{M}}(n|\mathbf{b}_{1:n-1})$. For time index n , (20) and (21) are repeated m -times.

The MMSE estimate of $\check{\mathbf{x}}(n)$ given $\mathbf{b}_{1:n}$ is $\hat{\check{\mathbf{x}}}(n|\mathbf{b}_{1:n}) = E\{\check{\mathbf{x}}(n)|\mathbf{b}_{1:n}\} = E\{\check{\mathbf{x}}(n)|\mathbf{b}_{1:n-1}, \mathbf{b}^{(1:m)}(n)\} = \hat{\check{\mathbf{x}}}^{(m)}(n|\mathbf{b}_{1:n-1})$. The corresponding ECM is $\check{\mathbf{M}}(n|\mathbf{b}_{1:n}) := \check{\mathbf{M}}^{(m)}(n|\mathbf{b}_{1:n-1})$.

The state estimates $\hat{\check{\mathbf{x}}}^{(i)}(n|\mathbf{b}_{1:n-1})$ in (14) are the first p components of the augmented state estimate $\hat{\check{\mathbf{x}}}^{(i)}(n|\mathbf{b}_{1:n-1})$, i.e., $\hat{\check{\mathbf{x}}}^{(i)}(n|\mathbf{b}_{1:n-1}) = [\hat{\check{\mathbf{x}}}^{(i)}(n|\mathbf{b}_{1:n-1})]_{1:p}$ and the noise estimate is the $(p+1)$ -st component.

Corollary 1 For $i = 1$, $E\{v(n)|\mathbf{b}_{1:n-1}, \mathbf{b}^{(1:i)}(n)\} \neq 0$.

Proof: The $(p+1)$ -st entry of $\hat{\check{\mathbf{x}}}^{(i)}(n|\mathbf{b}_{1:n-1})$ in (20) is the noise estimate $E\{v(n)|\mathbf{b}_{1:n-1}, \mathbf{b}^{(1:i)}(n)\}$. Thus, for $i = 1$

$$\begin{aligned} & E\{v(n)|\mathbf{b}_{1:n-1}, b(n)\} \\ &= E\{v(n)|\mathbf{b}_{1:n-1}\} + \sqrt{\frac{2}{\pi}} \frac{[\check{\mathbf{M}}^{(0)}(n|\mathbf{b}_{1:n-1})\check{\mathbf{h}}(n)]_{p+1}}{\sqrt{\check{\mathbf{h}}^T(n)\check{\mathbf{M}}^{(0)}(n|\mathbf{b}_{1:n-1})\check{\mathbf{h}}(n)}} b(n) \\ &= \sqrt{\frac{2}{\pi}} \frac{c_v(n)}{\sqrt{\check{\mathbf{h}}^T(n)\check{\mathbf{M}}(n|\mathbf{b}_{1:n-1})\check{\mathbf{h}}(n) + c_v(n)}} b(n) \neq 0. \end{aligned} \quad (22)$$

The last equality follows since $E\{v(n)|\mathbf{b}_{1:n-1}\} = E\{v(n)\} = 0$ and $[\check{\mathbf{M}}^{(0)}(n|\mathbf{b}_{1:n-1})\check{\mathbf{h}}(n)]_{p+1} = c_v(n)$. ■

The similarity of the m-IQKF in Proposition 1 and the clairvoyant KF based on un-quantized observations (cf. [P1]-[C1]) is quite remarkable. The ECM updates in (21) are identical to the ECM updates of the KF in (11) except for the scale factor $2/\pi$. The variance penalties associated with the m-IQKF are investigated in the following corollaries.

Corollary 2 Consider the m-IQKF algorithm in Proposition 1 and define the ECM reduction after $i = 1, \dots, m$ iterations as $\Delta\check{\mathbf{M}}_i(n) := \check{\mathbf{M}}^{(0)}(n|\mathbf{b}_{1:n-1}) - \check{\mathbf{M}}^{(i)}(n|\mathbf{b}_{1:n-1})$, where $\check{\mathbf{M}}^{(0)}(n|\mathbf{b}_{1:n-1}) := \check{\mathbf{M}}(n|\mathbf{b}_{1:n-1})$. With $c_i := 1 - (1 - \frac{2}{\pi})^i$, the error covariance reduction after i iterations is given as

$$\Delta\check{\mathbf{M}}_i(n) = c_i \frac{\check{\mathbf{M}}^{(0)}(n|\mathbf{b}_{1:n-1})\check{\mathbf{h}}(n)\check{\mathbf{h}}^T(n)\check{\mathbf{M}}^{(0)}(n|\mathbf{b}_{1:n-1})}{\check{\mathbf{h}}^T(n)\check{\mathbf{M}}^{(0)}(n|\mathbf{b}_{1:n-1})\check{\mathbf{h}}(n)} \quad (23)$$

Proof: We first write $\Delta\check{\mathbf{M}}_i(n)$ as a summation of differences between successive ECM matrices

$$\begin{aligned} \Delta\check{\mathbf{M}}_i(n) &:= \check{\mathbf{M}}^{(0)}(n|\mathbf{b}_{1:n-1}) - \check{\mathbf{M}}^{(i)}(n|\mathbf{b}_{1:n-1}) \\ &= \sum_{j=1}^i [\check{\mathbf{M}}^{(j-1)}(n|\mathbf{b}_{1:n-1}) - \check{\mathbf{M}}^{(j)}(n|\mathbf{b}_{1:n-1})] \\ &= \frac{2}{\pi} \sum_{j=1}^i \frac{\check{\mathbf{M}}^{(j-1)}(n|\mathbf{b}_{1:n-1})\check{\mathbf{h}}(n)\check{\mathbf{h}}^T(n)\check{\mathbf{M}}^{(j-1)}(n|\mathbf{b}_{1:n-1})}{\check{\mathbf{h}}^T(n)\check{\mathbf{M}}^{(j-1)}(n|\mathbf{b}_{1:n-1})\check{\mathbf{h}}(n)} \end{aligned} \quad (24)$$

where the last equality follows from (21). Next, we multiply

$\check{M}^{(i)}(n|\mathbf{b}_{1:n-1})$ from (21) by $\check{\mathbf{h}}(n)$ to obtain

$$\check{M}^{(i)}(n|\mathbf{b}_{1:n-1})\check{\mathbf{h}}(n) = \check{M}^{(i-1)}(n|\mathbf{b}_{1:n-1})\check{\mathbf{h}}(n) - \frac{2}{\pi} \frac{\check{M}^{(i-1)}(n|\mathbf{b}_{1:n-1})\check{\mathbf{h}}(n)\check{\mathbf{h}}^T(n)\check{M}^{(i-1)}(n|\mathbf{b}_{1:n-1})\check{\mathbf{h}}(n)}{\check{\mathbf{h}}^T(n)\check{M}^{(i-1)}(n|\mathbf{b}_{1:n-1})\check{\mathbf{h}}(n)} \quad (25)$$

$$= \left(1 - \frac{2}{\pi}\right) \check{M}^{(i-1)}(n|\mathbf{b}_{1:n-1})\check{\mathbf{h}}(n). \quad (26)$$

Repeating steps (25)-(26) for $\check{M}^{(i-1)}(n|\mathbf{b}_{1:n-1})\check{\mathbf{h}}(n)$ with decreasing index i yields $\check{M}^{(i)}(n|\mathbf{b}_{1:n-1})\check{\mathbf{h}}(n) = \left(1 - \frac{2}{\pi}\right)^i \check{M}^{(0)}(n|\mathbf{b}_{1:n-1})\check{\mathbf{h}}(n)$ which when substituted in (24) with $i = j - 1$, results in

$$\Delta \check{M}_i(n) = \frac{2}{\pi} \sum_{j=1}^i \left(1 - \frac{2}{\pi}\right)^{j-1} \frac{\check{M}^{(0)}(n|\mathbf{b}_{1:n-1})\check{\mathbf{h}}(n)\check{\mathbf{h}}^T(n)\check{M}^{(0)}(n|\mathbf{b}_{1:n-1})}{\check{\mathbf{h}}^T(n)\check{M}^{(0)}(n|\mathbf{b}_{1:n-1})\check{\mathbf{h}}(n)}.$$

Upon invoking the geometric sum identity $\frac{2}{\pi} \sum_{j=1}^i \left(1 - \frac{2}{\pi}\right)^{j-1} = 1 - \left(1 - \frac{2}{\pi}\right)^i$, (23) follows. ■

From the KF's ECM in (11), it follows readily that the ECM reduction for un-quantized observations $\check{M}(n|\mathbf{b}_{1:n-1}) - \check{M}(n|\mathbf{b}_{1:n})$ corresponds with $c_m = 1$ in (23). Therefore, the ECM reduction achieved by quantizing to m bits is c_m times smaller than the one achieved with analog-amplitude observations. Values of c_m are shown in Table I. With only 4 bits of quantization, the value of c_m is just 2% less than the value for the clairvoyant KF ($c_m = 1$).

From Corollary 2 we can relate the predicted MSE $\text{tr}\{\check{M}(n|\mathbf{b}_{1:n-1})\}$ and the corrected MSE $\text{tr}\{\check{M}(n|\mathbf{b}_{1:n})\}$ after observing the m -bits of n -th observation, $\mathbf{b}^{(1:m)}(n)$, i.e., $\check{M}(n|\mathbf{b}_{1:n}) = \check{M}(n|\mathbf{b}_{1:n-1}) - \Delta \check{M}_m(n)$. Substituting for $\Delta \check{M}_m(n)$ we obtain

$$\check{M}(n|\mathbf{b}_{1:n}) = \check{M}(n|\mathbf{b}_{1:n-1}) - c_m \frac{\check{M}(n|\mathbf{b}_{1:n-1})\check{\mathbf{h}}(n)\check{\mathbf{h}}^T(n)\check{M}(n|\mathbf{b}_{1:n-1})}{\check{\mathbf{h}}^T(n)\check{M}(n|\mathbf{b}_{1:n-1})\check{\mathbf{h}}(n)} \quad (27)$$

Equation (27) is instructive for understanding the MSE performance of m-IQKF since for $c_m = 1$, (27) coincides with the correction ECM of the KF in (11). Furthermore, $\lim_{m \rightarrow \infty} c_m \rightarrow 1$, implying that for infinite number of quantization bits we recover the clairvoyant KF. This important consistency result is summarized in the following corollary.

Corollary 3 *As the number of quantization bits $m \rightarrow \infty$, the correction step ECM at time n of the m-IQKF converges to the ECM of the clairvoyant KF given that $\mathbf{b}_{1:n-1} = \mathbf{y}_{1:n-1}$, i.e.,*

$$\lim_{m \rightarrow \infty} \check{M}^{(m)}(n|\mathbf{b}_{1:n-1}) = \check{M}(n|\mathbf{y}_{1:n}). \quad (28)$$

Proof: Since $\lim_{m \rightarrow \infty} c_m = \lim_{m \rightarrow \infty} [1 - (1 - \frac{2}{\pi})^m] = 1$, then for $c_m = 1$, $\check{M}^{(m)}(n|\mathbf{b}_{1:n-1})$ [cf. (27)] and $\check{M}(n|\mathbf{y}_{1:n})$ [cf. (11)] become identical, which results in (28). ■

Corollary 3 establishes that m-IQKF asymptotically (as the number of quantization bits increases) achieves the per correction step MSE performance of the clairvoyant KF. As demonstrated by simulations in Section IV, even a small number of quantization bits ($m = 2$ or $m = 3$) renders the MSE performance of m-IQKF indistinguishable from that of the clairvoyant KF.

TABLE I
PER STEP FACTOR, c_m , AND NOISE PENALTY FACTOR FOR IQKF

bits, m	1	2	3	4
c_m	0.637=2/π	0.868	0.952	0.983
$(1/c_m - 1)100\%$	57.08%	15.21%	5.04%	1.77%

B. Performance analysis of the m-IQKF

In the previous section, we quantified the *per correction step* ECM reduction $\Delta \check{M}_m(n)$ in the m-IQKF as a function of the number of bits m used for iteratively quantizing the observations $y(n)$. We next compare MSE performance of m-IQKF with that of the clairvoyant KF, when both prediction and correction steps are considered, by deriving the continuous-time Algebraic Riccati Equations (ARE) for both filters.

Consider first the discrete time ARE for the m-IQKF [P2]-[C2]. To simplify notation let $\check{M}(n+1) := \check{M}(n+1|\mathbf{b}_{1:n})$, $\check{M}(n) := \check{M}(n|\mathbf{b}_{1:n-1})$, $\check{M}(n+1) := \check{M}(n+1|\mathbf{b}_{1:n})$, $\check{M}(n) := \check{M}(n|\mathbf{b}_{1:n-1})$, and substitute (27) in (19) to obtain the m-IQKF ARE for the ECM of $\check{\mathbf{x}}(n)$ as

$$\check{M}(n+1) = \check{A}(n+1)\check{M}(n)\check{A}^T(n+1) + \mathbf{C}_{\check{u}}(n+1) - c_m \frac{\check{A}(n+1)\check{M}(n)\check{\mathbf{h}}(n)\check{\mathbf{h}}^T(n)\check{M}(n)\check{A}^T(n+1)}{\check{\mathbf{h}}^T(n)\check{M}(n)\check{\mathbf{h}}(n)}. \quad (29)$$

Substituting for $\check{A}(n+1)$, $\mathbf{C}_{\check{u}}(n+1)$, $\check{\mathbf{h}}(n)$ and $\check{M}(n)$ in (29), and writing only the leading $p \times p$ sub-matrices of the resulting expression, yields the ARE for the ECM of $\mathbf{x}(n)$ as

$$\mathbf{M}(n+1) = \mathbf{A}(n+1)\mathbf{M}(n)\mathbf{A}^T(n+1) + \mathbf{C}_{\mathbf{u}}(n+1) - c_m \frac{\mathbf{A}(n+1)\mathbf{M}(n)\mathbf{h}(n)\mathbf{h}^T(n)\mathbf{M}(n)\mathbf{A}^T(n+1)}{\mathbf{h}^T(n)\mathbf{M}(n)\mathbf{h}(n) + c_v(n)}. \quad (30)$$

Interestingly, the resulting ARE for the ECM of the m-IQKF [cf. (30)] becomes identical to the ARE of the clairvoyant KF [6, Chapter 5.11] as $\lim_{m \rightarrow \infty} c_m = 1$. The implication of these relations follows from the continuous-time ARE for the m-IQKF given in Proposition 2.

Proposition 2 *The continuous-time ECM $\mathbf{M}_c(t) = \mathbf{M}_c(nT_s) := \lim_{T_s \rightarrow 0} \check{M}(n; T_s)$ for the m-IQKF of (18)-(21) is the solution of the following differential (Riccati) equation:*

$$\dot{\mathbf{M}}_c(t) = \mathbf{A}_c(t)\mathbf{M}_c(t) + \mathbf{M}_c(t)\mathbf{A}_c^T(t) + \mathbf{C}_{\mathbf{u}}(t) - \mathbf{M}_c(t)\mathbf{h}_c(t) \left[\frac{c_{v_o}(t)}{c_m} \right]^{-1} \mathbf{h}_c^T(t)\mathbf{M}_c(t). \quad (31)$$

Proof: The derivation steps from (30) to (31) are the same as those followed for deriving the KF Riccati equation from the corresponding ECMs [6, pp. 259]. The only difference is that the scale factor, c_m , in (30) equals 1 in the case of the KF. ■

From the clairvoyant KF ARE [6, pp. 259]

$$\dot{\mathbf{M}}_c^K(t) = \mathbf{A}_c(t)\mathbf{M}_c^K(t) + \mathbf{M}_c^K(t)\mathbf{A}_c^T(t) + \mathbf{C}_{\mathbf{u}}(t) - \mathbf{M}_c^K(t)\mathbf{h}_c(t) [c_{v_o}(t)]^{-1} \mathbf{h}_c^T(t)\mathbf{M}_c^K(t) \quad (32)$$

where $\mathbf{M}_c^K(t)$ denotes the continuous-time ECM of KF, it is evident that the variance of the continuous-time observation noise of the m-IQKF is amplified by $1/c_m$ compared to that of the clairvoyant KF. This is the price paid for using quantized observations, $b(n)$, instead of the analog-amplitude ones, $y(n)$. In Table I the percentage observation noise variance increase $(1/c_m - 1)100\%$ versus number of quantization bits, m is shown.

IV. SIMULATIONS

The two-dimensional state space model simulated is

$$\dot{\mathbf{x}}_c(t) := \begin{pmatrix} \dot{x}_{c_1}(t) \\ \dot{x}_{c_2}(t) \end{pmatrix} = \begin{pmatrix} 0 & 1 \\ 0 & 0 \end{pmatrix} \begin{pmatrix} x_{c_1}(t) \\ x_{c_2}(t) \end{pmatrix} + \begin{pmatrix} 0 \\ 1 \end{pmatrix} u_c(t).$$

Noisy measurements at sensor S_k are given as $y_k(t) = x_{c_1}(t) + \theta_k x_{c_2}(t) + v_k(t)$ where θ_k is a parameter at sensor k . A discrete-time equivalent model is used with sampling time $T_s = 1$.

WSN data corresponding to $K = 2$ sensors with $[\theta_1 \ \theta_2] = [0.1 \ 0.2]$ are simulated. The measurement and state driving noise variances are $c_v(t) = 1$ and $c_u(t) = 1$. The MSE plots in Fig. 1 and Fig. 2 illustrate the evolution of the MSEs, obtained from the trace of the respective ECMs, against the time index n .

In the first simulation setup, Fig. 1, the MSE of the IQKF, given by $\text{tr}\{\mathbf{M}(n|\mathbf{b}_{1:n})\}$, is compared to the MSE of the clairvoyant KF. The simulations for IQKF are performed for 1, 2 and 3 bits. The plots demonstrate that there is a substantial MSE reduction when going from 1 bit of quantization to 2 bits and little MSE reduction for higher number of quantization bits. With 2 bits of quantization the MSE of IQKF is virtually coincident with that of the clairvoyant KF as was postulated by the analytical values in Table I whereby $c_2 = 86.8\%$.

Model consistency checks comparing the empirically obtained MSEs with analytical MSEs are shown in Fig. 2. Note that the analytical MSE is obtained from the trace of the ECM $\mathbf{M}(n|\mathbf{b}_{1:n}) := \mathbb{E}\{[\mathbf{x}(n) - \hat{\mathbf{x}}(n|\mathbf{b}_{1:n})][\mathbf{x}(n) - \hat{\mathbf{x}}(n|\mathbf{b}_{1:n})]^T | \mathbf{b}_{1:n}\}$. The empirical MSE is the sample estimator of $\text{tr}\{\mathbf{M}(n|\mathbf{b}_{1:n})\}$ obtained as a sample average of the squared estimation errors. The plots depict both predictor MSE $\text{tr}\{\mathbf{M}(n|\mathbf{b}_{1:n-1})\}$ and estimator MSE $\text{tr}\{\mathbf{M}(n|\mathbf{b}_{1:n})\}$. The consistency check reveals that the empirical and analytical MSEs are nearly identical.

Fig. 3 shows alternative model consistency tests for the IQKF using the normalized estimation error squared (NEES) tests of [1, Ch. 5.4]. NEES $r(n) := [\mathbf{x}(n) - \hat{\mathbf{x}}(n|\mathbf{b}_{1:n})]^T [\mathbf{M}(n|\mathbf{b}_{1:n})]^{-1} [\mathbf{x}(n) - \hat{\mathbf{x}}(n|\mathbf{b}_{1:n})]$ is postulated to have a χ^2 pdf with p degrees of freedom (since the p -dimensional $\tilde{\mathbf{x}}(n) := \mathbf{x}(n) - \hat{\mathbf{x}}(n|\mathbf{b}_{1:n})$ is assumed zero-mean Gaussian with covariance $\mathbf{M}(n|\mathbf{b}_{1:n})$ if the estimator is consistent with the model). Under the hypothesis that the estimator is consistent, L realizations of the NEES statistics $\{r_i(n)\}_{i=1}^L$ each χ^2 distributed with p degrees of freedom, lead to a χ^2 distribution with Lp degrees of freedom. This is checked by running Monte Carlo simulations and computing the sample average NEES $\hat{r}(n) := \frac{1}{L} \sum_{i=1}^L r_i(n)$ and then defining an acceptance (confidence) region (for the consistent hypothesis). If $l \leq \hat{r}(n) \leq u$, then the estimator is consistent; lower and upper bounds l and u are obtained from $\Pr\{\hat{r}_n \in [l, u]\} = 1 - \alpha$, where $1 - \alpha$ is the probability of acceptance region. Using $L = 50$ realizations, 200 time samples, a state space of $p = 2$ dimensions, and $\alpha = 0.05$ (i.e., 95% region), we observed that indeed only 7% of the 100 time samples lie outside the 95% acceptance region.

V. CONCLUDING REMARKS

Recursive state estimation based on quantized observations was considered. Multi-bit quantization was done using iterative binary quantizing of the measurement innovations. Joint quantization and estimation was used to develop a Kalman-like algorithm.

Motivated by the need to find quantifiable trade-offs between estimation performance and number of quantization bits for

distributed estimation, it was shown that quantization using 2 to 3 bits improves the performance of the Kalman-like algorithm to virtually coincide with the optimal state estimator (Kalman filter), with only minimal increase in computation. This result was corroborated by simulation results. It was further shown through simulations that true filter covariances are consistent with analytical ones¹.

REFERENCES

- [1] Y. Bar-Shalom and X. Li, *Estimation and Tracking: Principles, Techniques, and Software*. Artech House, 1993.
- [2] P. Djuric, J. Kotecha, J. Zhang, Y. Huang, T. Ghirmai, M. Bugallo, and J. Miguez, "Particle filtering," *IEEE Sig. Proc. Mag.*, vol. 20, pp. 19–38, Sep. 2003.
- [3] R. M. Gray, "Quantization in task-driven sensing and distributed processing," in *Proc. Int. Conf. Acoustics, Speech, Signal Processing*, vol. 5, pp. V-1049–V-1052, Toulouse, France, May 14-19, 2006.
- [4] S. Julier and J. Uhlmann, "Unscented filtering and nonlinear estimation," *Proc. IEEE*, vol. 92, pp. 401–422, Mar. 2004.
- [5] J. Kotecha and P. Djuric, "Gaussian particle filtering," *IEEE Trans. on Sig. Processing*, vol. 51, pp. 2602–2612, Oct. 2003.
- [6] P. S. Maybeck, *Stochastic Models, Estimation and Control – Vol. 1*. Academic Press, 1979.
- [7] H. Papadopoulos, G. Wornell, and A. Oppenheim, "Sequential signal encoding from noisy measurements using quantizers with dynamic bias control," *IEEE Trans. on Infor. Theory*, vol. 47, pp. 978–1002, 2001.
- [8] A. Ribeiro, G. B. Giannakis, and S. I. Roumeliotis, "SOI-KF: Distributed Kalman filtering with low-cost communications using the sign of innovations," *IEEE Trans. on Sig. Proc.*, vol. 54, no. 12, pp. 4782–4795, Dec 2006.

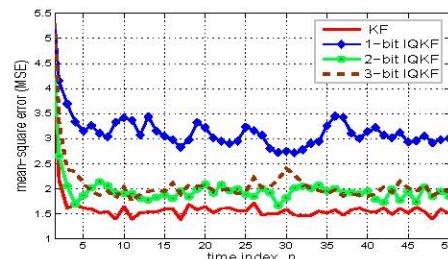


Fig. 1. IQKF estimator MSE $\text{tr}\{\mathbf{M}(n|\mathbf{b}_{1:n})\}$ from Monte Carlo data for 1-3 bits of quantization; MSE for clairvoyant KF is included for comparison.

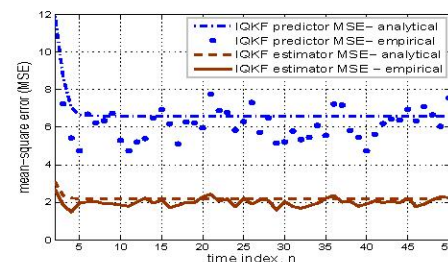


Fig. 2. Comparing empirical MSE from Monte Carlo data and analytical MSE, for predictor ECM $\mathbf{M}(n|\mathbf{b}_{1:n-1})$ and estimator ECM $\mathbf{M}(n|\mathbf{b}_{1:n})$.

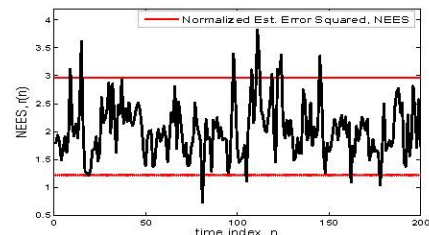


Fig. 3. Consistency test using normalized estimation error squared (NEES), $r(n)$, compared with the 95% probability region using 2 bits of quantization.

¹The views and conclusions contained in this document are those of the authors and should not be interpreted as representing the official policies of the Army Research Laboratory or the U. S. Government.